A simplified dynamic bioenergetic model for coral-*Symbiodinium* symbioses

Ross Cunning[a,*], Erik B. Muller[b], Ruth D. Gates[a], Roger M. Nisbet[b]

[a] *Hawaii Institute of Marine Biology, Kaneohe, HI 96744, USA*

[b] *Department of Ecology, Evolution, and Marine Biology, Santa Barbara, CA 93106, USA*

Abstract

This is the abstract.

Introduction

The nutritional exchange between corals and *Symbiodinium* directly underlies the capacity of corals to build coral reef ecosystems, worth trillions of US Dollars annually (Costanza, Groot, and Sutton 2014). However, the complex symbiotic metabolism of corals is vulnerable to disruption by numerous anthropogenic environmental perturbations, jeopardizing their future persistence. In order to understand and predict coral responses to complex changes in their environment, a mechanistic understanding of how multiple interacting factors drive the individual and emergent physiology of both symbiotic partners is necessary. Such a task is well suited for theoretical modeling frameworks such as Dynamic Energy Budget (DEB) theory (Kooijman 2010), although the complexity of such theory makes these efforts inaccessible to many biologists (Jager, Martin, and Zimmer 2013). In order to bridge this gap, we present here a simplified dynamic bioenergetic model for coral-*Symbiodinium* symbioses that aims to mechanistically integrate the impacts of complex environmental change on the physiological performance of reef corals, including responses to environmental stress.

In reef coral symbioses, intracellular *Symbiodinium* translocate photosynthetically fixed carbon to support coral metabolism, while the animal host provides access to inorganic nutrients and carbon dioxide (Muscatine and Porter 1977). Previous application of DEB theory to this syntrophic system (Muller et al. 2009) demonstrated a stable symbiotic relationship and qualitatively realistic growth and biomass ratios across gradients of ambient irradiance, nutrients, and food. This model assumed that 1) *Symbiodinium* has priority access to fixed carbon through photosynthesis, 2) the coral animal has priority access to dissolved nitrogen through contact with seawater, and 3) each partner shares with the other only what it cannot use for its own growth. In its simplest form, this principle of sharing the surplus is sufficient to describe the dynamics of diverse syntrophic organs and organisms (e.g., trees, duckweeds, corals), suggesting the mechanism is mathematically and evolutionarily robust (Nisbet et al., in prep.).

While the formal DEB model of Muller et al. (2009) represents the most significant theoretical contribution in coral symbiosis research to date, we aim to strengthen the role of theory and broaden its potential application in three primary ways:

1. *Develop a detailed module of environmental stress.* Of primary interest to coral biologists and ecologists is symbiosis dysfunction under environmental stress, resulting in coral "bleaching"–the loss of algal symbionts from the association (Jokiel and Coles 1977). Photooxidative stress in *Symbiodinium* is considered a primary trigger of bleaching in response to high temperature and/or light (Weis 2008), and prolonged or severe bleaching can result in mortality, though corals sometimes recover their symbionts. Bleaching susceptibility, severity, and recovery may by influenced by interacting factors such as heterotrophy and

*Corresponding Author
Email address: ross.cunning@gmail.com (Ross Cunning)

nutrient availability (Wooldridge 2014b), and the genetic identity of *Symbiodinium* (Glynn et al. 2001). To simulate these bleaching-related phenomena, we develop a generalized framework linking overreduction of the photosynthetic light reactions to downstream impacts of photoinhibition and photodamage.

2. *Reduce theoretical and mathematical complexity.* Following the logic of Jager, Martin, and Zimmer (2013), we exclude certain features of formal DEB models in order to capture behaviors of interest with the simplest possible formulation. Here, we present a model without reserves, maturity, or reproduction (see Kooijman 2010). This formulation restricts the model's scope to the bioenergetics of growth and symbiosis dynamics in adult corals (i.e., reproduction, larval stages, and metamorphosis are not considered), but greatly reduces theoretical complexity and parameter numbers, which is advantageous given the relative paucity of data for corals. However, our primary motivation for reducing complexity was to increase accessibility and applicability for biologists and ecologists without requiring significant expertise in DEB theory.
3. *Provide well-documented, open-access code.* In order to facilitate the continued development and application of theoretical modeling tools for coral symbioses, we provide open access to the model in the form of detailed, commented code written in the R language (R Core Team 2014). With an accessible and modular framework, we envision this as a resource for futher development by the scientific community to include additional complexity and problem-specific components. To widen the audience for this work, we chose the R language because it is freely available and in common use by biologists and ecologists.

With these as our primary motivations, we describe a simplified approach to dynamic bioenergetic modeling of coral-algal symbioses that tracks carbon and nitrogen acquisition and sharing between partners. This theoretical framework dynamically integrates the influence of external irradiance, nutrients, and prey availability on coral growth and symbiosis dynamics (i.e., symbiont:host biomass ratios), allowing for the possibility of coral bleaching in the event of photooxidative stress. In the following sections, we describe the formulation of this model and justify its structure and parameter values based on relevant literature. We then demonstrate the model's behavior and discuss some of its major implications and outcomes, and the wide range of potential applications for this model in the study of cnidarian-algal symbioses.

Model description

In this dynamic bioenergetic model of coral-algal symbiosis, carbon and nitrogen are acquired by each partner and used to construct biomass. A graphical representation of the model is presented in Fig. 1, and each model flux and parameter are defined in Tables 1 and 2, respectively. We use C-moles as the unit of biomass for consistency with the rigorous mass balance of DEB theory: 1 C-mole is equivalent to the amount of biomass containing 1 mole of Carbon atoms. Host biomass (H), symbiont biomass (S), and prey biomass (X) have fixed, but different, molar N:C ratios (Table 2). Carbon and nitrogen are combined to produce biomass by synthesizing units (SU), which are mathematical specifications of the formation of a product from two substrates; we use the parallel complementary formulation of Kooijman (2010) to specify these fluxes. The two state variables are symbiont biomass and coral biomass; because resources are acquired proportionally to surface area, and surface area is proportional to volume (i.e., corals are "V1-morphs" in DEB terminology (Kooijman 2010)), biomass increases exponentially during growth (indeed, corals grow exponentially (Bak 1976)). The specific growth rate and the ratio of symbiont to host biomass are the responses of interest of the system. Below we describe the formulation of each flux involved in producing these responses.

Table 1. Model fluxes

Symbol	Description	Units	Eq. no.
j_X	Prey uptake rate	molX CmolH^{-1} d^{-1}	3
j_N	Nitrogen uptake rate	molN CmolH^{-1} d^{-1}	4
j_{HG}	Host biomass formation rate	CmolH CmolH^{-1} d^{-1}	5
r_{NH}	Recycled nitrogen from host turnover	molN CmolH^{-1} d^{-1}	6
ρ_N	Nitrogen shared with the symbiont	molN CmolH^{-1} d^{-1}	7
j_L	Light absorption rate	molph CmolS^{-1} d^{-1}	9
j_{CO_2}	CO_2 input to photosynthesis	molCO_2 CmolH^{-1} d^{-1}	10

Symbol	Description	Units	Eq. no.
r_{CH}	Recycled CO_2 from host turnover	molCO$_2$ CmolH^{-1} d^{-1}	11
r_{CS}	Recycled CO_2 from symbiont turnover	molCO$_2$ CmolS^{-1} d^{-1}	12
j_{CP}	Photosynthesis rate	molC CmolS^{-1} d^{-1}	13
j_{eL}	Light energy in excess of photochemistry	molph CmolS^{-1} d^{-1}	14
j_{NPQ}	Total capacity of NPQ	molph CmolS^{-1} d^{-1}	15
c_{ROS}	ROS production proportional to baseline	–	16
r_{NS}	Recycled nitrogen from symbiont turnover	molN CmolS^{-1} d^{-1}	17
j_{SG}	Symbiont biomass formation rate	CmolS CmolS^{-1} d^{-1}	18
ρ_C	Fixed carbon shared with host	molC CmolS^{-1} d^{-1}	19
j_{ST}	Symbiont turnover rate	CmolS CmolS^{-1} d^{-1}	20

Table 2. Model parameters

Symbol	Description	Value	Units
n_{NH}	N:C molar ratio in host biomass	0.19	–
n_{NS}	N:C molar ratio in symbiont biomass	0.2	–
n_{NX}	N:C molar ratio in prey biomass	0.13	–
j^0_{HT}	Specific turnover rate of host biomass	0.03	CmolH CmolH^{-1} d^{-1}
j^0_{ST}	Specific turnover rate of symbiont biomass	0.03	CmolS CmolS^{-1} d^{-1}
σ_{NH}	Proportion host nitrogen turnover recycled	0.9	–
σ_{CH}	Proportion host carbon turnover recycled	0.9	–
σ_{NS}	Proportion symbiont nitrogen turnover recycled	0.9	–
σ_{CS}	Proportion symbiont carbon turnover recycled	0.9	–
j_{Xm}	Maximum specific feeding rate of host	0.1292	molX CmolH^{-1} d^{-1}
K_X	Half-saturation constant for prey uptake by host	20e-6	molX L^{-1}
j_{Nm}	Maximum specific DIN uptake rate by host	0.048	molN CmolH^{-1} d^{-1}
K_N	Half-saturation constant for DIN uptake by host	0.46e-6	molN L^{-1}
$j^p_{CO_2}$	Passive CO_2 delivery to symbiont	4.04e-3	molC CmolH^{-1} d^{-1}
$j^a_{CO_2}$	Active CO_2 delivery to symbiont	0.32–18.0	molC CmolH^{-1} d^{-1}
j_{HGm}	Maximum specific growth rate of host	1	CmolH CmolH^{-1} d^{-1}
n_{LC}	Quantum yield of photosynthesis	0.1	molC mol ph^{-1}
$\bar{a}^*$	Effective light-absorbing cross-section of symbiont	1.34	m^2 CmolS^{-1}
k_{NPQ}	NPQ capacity of symbiont, relative to C-fixation	4	–
k_{ROS}	Excess photon energy that doubles ROS production, relative to baseline levels	40-80	mol ph CmolS^{-1} d^{-1}
k	Exponent on ROS production rate	1	–
j_{CPm}	Maximum specific photosynthesis rate of symbiont	2.8	molC CmolS^{-1} d^{-1}
j_{SGm}	Maximum specific growth rate of symbiont	0.25	CmolS CmolS^{-1} d^{-1}
b	Scaling parameter for strength of bleaching response	3	–

State equations

The balance equations for symbiont and host biomass are expressed as:

$$\frac{dS}{Sdt} = j_{SG} - j_{ST} \tag{1}$$

$$\frac{dH}{Hdt} = j_{HG} - j^0_{HT} \tag{2}$$

These are expressed per unit of symbiont and host biomass, respectively. The specific biomass growth and turnover rates that define these balance equations are produced by combinations of the individual model fluxes (see Table 1 for definitions and units), which are each expressed as mass-specific rates (e.g., per C-mole of symbiont or host biomass). When necessary, conversions between symbiont-mass-specific and host-mass-specific rates are accomplished by multiplying or dividing by the symbiont:host biomass ratio.

Coral animal fluxes

The coral animal acquires both carbon and nitrogen from feeding on prey from the environment. Prey acquisition is specified by Michaelis-Menten kinetics (i.e., a Holling type II function) with a maximum feeding rate j_{Xm} and half-saturation constant K_X:

$$j_X = \frac{j_{Xm} \cdot X}{X + K_X} \tag{3}$$

Additionally, the coral animal acquires nitrogen dissolved in the surrounding seawater, which is assumed to represent ammonium, the primary form utilized by corals (Yellowlees, Rees, and Leggat 2008). This gives the host (rather than the symbiont) priority in nitrogen utilization; this capacity is supported by experimental evidence (Wang and Douglas 1998) and is consistent with the physical arrangment of the partners, where the host is in direct contact with the external environment. The uptake of nitrogen from the environment is thus specified by Michaelis-Menten kinetics using a maximum uptake rate j_{Nm} and half-saturation constant K_N:

$$j_N = \frac{j_{Nm} \cdot N}{N + K_N} \tag{4}$$

Coral biomass formation is then specified by a parallel complementary SU that combines carbon and nitrogen, according to:

$$j_{HG} = \left(\frac{1}{j_{HGm}} + \frac{1}{\rho_C \frac{S}{H} + j_X} + \frac{1}{(j_N + n_{NX} j_X + r_{NH})/n_{NH}} - \frac{1}{\rho_C \frac{S}{H} + j_X + (j_N + n_{NX} j_X + r_{NH})/n_{NH}} \right)^{-1} \tag{5}$$

where ρ_C is the surplus fixed carbon shared by the symbiont (see below), and r_{NH} is the recycled portion of the nitrogen liberated by host biomass turnover:

$$r_{NH} = \sigma_{NH} j^0_{HT} \tag{6}$$

The amount of nitrogen input to the coral biomass SU in excess of what is actually consumed in biomass formation (i.e., surplus nitrogen, or the rejection flux[1] of the SU) is then made available to the symbiont:

$$\rho_N = (j_N + n_{NX} j_X + r_{NH} - n_{NH} j_{HG})_+ \tag{7}$$

Due to the inherent inefficiency of the parallel complementary SU formulation, there is always some nitrogen shared with the symbiont even when coral biomass formation is strongly nitrogen-limited. Likewise, there is always a non-zero rejection flux of carbon from the coral biomass SU, which is assumed to be lost to the environment.

[1] Rejection fluxes must always be positive, and hence are specified with the notation $(x)_+$, which means $max(x, 0)$.

Symbiodinium *fluxes*

The symbiont produces fixed carbon through photosynthesis, a process represented here by a single SU with two substrates: light (photons) and inorganic carbon (CO_2). The amount of light absorbed by the symbiont depends on the scalar irradiance at the site of light absorption, which is modified substantially relative to external downwelling irradiance owing to multiple scattering by the coral skeleton and self-shading by surrounding symbionts (Enríquez, Méndez, and Iglesias-Prieto 2005; Marcelino et al. 2013). We used data from Marcelino et al. (2013) to empirically derive an "amplification factor" A (the ratio of internal scalar irradiance to external downwelling irradiance) as a function of symbiont density (expressed as symbiont to host biomass ratio), which is specified as:

$$A = 1.26 + 1.39 \cdot \exp(-6.48 \cdot \frac{S}{H}) \tag{8}$$

This amplification factor is then multiplied by the external downwelling irradiance L and the effective light-absorbing surface area of symbiont biomass $\bar{a}^*$ to specify the total amount of light absorbed:

$$j_L = A \cdot L \cdot \bar{a}^* \tag{9}$$

We then specify two pathways for input of inorganic carbon to the photosynthesis SU: 1) passive diffusion of CO_2 from the external environment ($j^p_{CO_2}$), and 2) active delivery of CO_2 to the symbiont by the host ($j^a_{CO_2}$). The passive flux ensures that some CO_2 is always available to photosynthesis, and the active flux encompasses potentially diverse mechanisms by which the host may enhance CO_2 availability for the symbiont, including active transport of bicarbonate, carbonic anhydrase-catalyzed conversion of bicarbonate to CO_2 to promote diffusion toward the symbiont (Tansik, Fitt, and Hopkinson 2015), and acidification of the symbiosome to increase localized CO_2 concentrations around the symbiont (Barott et al. 2014). Since the host physically separates the symbiont from the external environment, both the passive and active flux rates are proportional to host biomass. A more rigorous, mechanistic model of inorganic carbon processing would require spatially explicit internal pools accounting for pH and carbon speciation, which is beyond the current scope of this work. Instead, the specification of fixed passive and active CO_2 input rates, $j^p_{CO_2}$ and $j^a_{CO_2}$, offers the user the opportunity to compare different rates of CO_2 delivery that may characterize different coral species (Wooldridge 2014a). The input of CO_2 to the photosynthesis SU is therefore specified as:

$$j_{CO_2} = j^p_{CO_2} + j^a_{CO_2} \tag{10}$$

Additional metabolic CO_2 recycled from both the host and symbiont biomass turnover is also made available to the photosynthesis SU, according to:

$$r_{CH} = \sigma_{CH} j^0_{HT} \tag{11}$$

$$r_{CS} = \sigma_{CS} j^0_{ST} \tag{12}$$

Fixed carbon is then produced by the photosynthesis SU according to:

$$j_{CP} = \left(\frac{1}{j_{CPm}} + \frac{1}{n_{LC} j_L} + \frac{1}{(j_{CO_2} + r_{CH})\frac{H}{S} + r_{CS}} - \frac{1}{n_{LC} j_L + (j_{CO_2} + r_{CH})\frac{H}{S} + r_{CS}} \right)^{-1} \cdot c^{-1}_{ROS} \tag{13}$$

where j_{CPm} is the maximum specific rate of photosynthesis, and c_{ROS} is the relative rate of reactive oxygen species production (see below). Dividing the photosynthetic rate by c_{ROS} causes a decline in response to photooxidative stress (i.e., photoinhibition).

Light energy absorbed in excess of what is used to fix carbon is specified by the SU "rejection flux", according to:

$$j_{eL} = (j_L - j_{CP}/n_{LC})_+ \tag{14}$$

This excess light energy must be quenched by alternative pathways in order to prevent photooxidative damage (Powles 1984). *Symbiodinium* utilize a variety of pathways for non-photochemical quenching (NPQ; Roth 2014), which we collect in a relative NPQ capacity specified as a parameter of the symbiont (k_{NPQ}). NPQ capacity may also be susceptible to reduction by photoinhibition, so the total NPQ capacity is specified as:

$$j_{NPQ} = k_{NPQ} \cdot c_{ROS}^{-1} \tag{15}$$

If light energy further exceeds the total capacity of both carbon fixation and NPQ, then reactive oxygen species (ROS) are produced. We represent this as a relative quantity c_{ROS}, which takes a value of 1 when all light absorbed can be quenched by photochemistry and NPQ, and increases as the amount of excess excitation energy further increases:

$$c_{ROS} = 1 + \left(\frac{(j_{eL} - j_{NPQ})_+}{k_{ROS}} \right)^k \tag{16}$$

where k_{NPQ}, k_{ROS}, and k are parameters of the symbiont that determine the onset and rate of ROS production. Importantly, c_{ROS} as specified here is not a function of absolute light absorption, but rather the amount of excess light energy, j_{eL}, after accounting for carbon fixation and NPQ. A direct consequence of this formulation is that CO_2-limitation of photosynthesis can lead to ROS production, an important mechanism (Wooldridge 2009) that was not captured by previous representations of photooxidative stress (Eynaud, Nisbet, and Muller 2011). Moreover, this formulation allows functional diversity among symbiont types to be explored by changing the parameters k_{NPQ}, k_{ROS}, and k.

Carbon fixed by photosynthesis (j_{CP}) is then combined with nitrogen shared by the host (ρ_N) and nitrogen recycled from symbiont biomass turnover

$$r_{NS} = \sigma_{NS} j_{ST}^0 \tag{17}$$

to build new symbiont biomass, following the SU equation:

$$j_{SG} = \left(\frac{1}{j_{SGm}} + \frac{1}{j_{CP}} + \frac{1}{(\rho_N \frac{H}{S} + r_{NS})/n_{NH}} - \frac{1}{j_{CP} + (\rho_N \frac{H}{S} + r_{NS})/n_{NH}} \right)^{-1} \tag{18}$$

The rejection flux of carbon from this SU represents the amount of fixed carbon produced by photosynthesis in excess of what can be used to produce symbiont biomass; this surplus, ρ_C, is translocated to the coral host:

$$\rho_C = (j_{CP} - j_{SG})_+ \tag{19}$$

The rejection flux of nitrogen from the symbiont biomass SU is lost to the environment.

Symbiont biomass turnover includes a component of constant turnover specified by the parameter j_{ST}^0, representing fixed maintenance costs, plus a component that scales with the magnitude of ROS production.

$$j_{ST} = j_{ST}^0 (1 + b(c_{ROS} - 1)) \tag{20}$$

This second component of symbiont biomass loss can represent both photodamage and/or symbiont expulsion (i.e., bleaching), both of which occur in response to high levels or ROS production. The parameter b is included to scale biomass loss due to bleaching in response to ROS. (Note that recycling of symbiont biomass turnover (rNS and rCS) only occurs based on the maintenance component of turnover (i.e., j_{ST}^0), and not the bleaching-related component, as this loss represents biomass that is damaged or expelled from the host).

Numerical analysis

A time-stepping Euler method was used to solve the state equations since the production and rejection fluxes of the SUs are imiplicitly defined. Specifically, the rejection fluxes of carbon and nitrogen from the symbiont and host biomass SUs act as reciprocal input fluxes to the other SU. In addition, the rejection flux of excitation energy from the photosynthesis SU acts to reduce its own production flux (i.e., photoinhibition), and hence a discretized time-stepping procedure was necessary. A vector of time values was created for each simulation run, along which dynamic environmental forcing functions (irradiance, DIN, and prey abundance) can be designed. These vectors, along with initial values of symbiont and host biomass, then serve as input to the time-stepping function, which solves for the current system state using values of the previous system state where necessary. A time step of 0.1 days was used for all simulations, which were performed using R code that is available in the data repository accompanying this article: github.com/jrcunning/Rcoral.

To aid in visualizing model results, we calculated values to indicate the degree to which product formation at an SU was limited by availability of either of its two substrates:

$$\log\left(\frac{\min(j_{S1}, j_{Pm})}{\min(j_{S2}, j_{Pm})}\right) \tag{21}$$

where j_{S1} and j_{S2} are the specific input fluxes of the two substrates and j_{Pm} is the maximum specific product formation rate, all with units of Cmol Cmol^{-1} d^{-1}.

Sensitivity analysis

Each default parameter value used in the model (Table 2) is based on carefully selected relevant literature. A supplementary document detailing the derivations of each of these default parameter values is provided. Nevertheless, it is important to evaluate the sensitivity of the model to changes in these parameter values. We measured fractional change in steady state values in response to fractional change in parameter values, relative to their default values (Table 2).

Steady state behavior

To analyze qualitative behavior, we ran the model to steady state across gradients of external irradiance and nutrients (Fig. 2), which revealed patterns consistent with observed phenomena in corals. Predicted growth rates are low at low light and DIN, and begin increasing as both of these factors increase (Fig. 2A). Low light is limiting to photosynthesis (Fig. 2D), which leads to carbon-limitation of host growth (Fig. 2B) and an associated increase in the symbiont to host biomass ratio (Fig. 2C). In agreement with this trend are many observations of negative correlation between irradiance and symbiont density (Stimson 1997; Brown et al. 1999; Fitt et al. 2000; Titlyanov et al. 2001). As higher light alleviates light-limitation of photosynthesis, growth becomes less carbon-limited. Similarly, elevating DIN up to ~2 µM alleviates nitrogen-limitation (Fig. 2B). Increased growth at higher DIN is predicted by the DEB model of Muller et al. (2009), and has also been observed experimentally (Muller-Parker et al. 1994; Tanaka et al. 2007; Tanaka et al. 2013). However, DIN elevation beyond a certain point (e.g., 2-3 µM in these simulations) has little effect on growth as carbon becomes limiting (Fig. 2B). Very high nutrient levels may even reduce growth (Shantz, Lemoine, and Burkepile 2015), although these impacts are not likely to occur within the range of concentrations considered here (<4 µM) (Ferrier-Pagès et al. 2000).

In addition to increasing growth, DIN also increases the symbiont to host biomass ratio, a phenomenon also observed in reef corals (Marubini and Davies 1996). S:H ratios also increase under low light (Stimson 1997; Fitt et al. 2000; Anthony and Hoegh-Guldberg 2003). At low DIN and intermediate light, more typical of coral reef environments, symbiont to host biomass ratios are around ~0.1-0.3, which is consistent with values reported in the literature (Muscatine, R McCloskey, and E Marian 1981; Edmunds et al. 2011).

The maximum predicted growth rates of ~0.1 d^{-1}, occurring between ~10-15 mol photons m^{-2} s^{-1} light and >~3 µM DIN (Fig. 2A), are comparable to the rate of 0.07 d^{-1} measured by Tanaka et al. (2007) under similar

N-enriched conditions. Growth under conditions more typical of reef environments (<0.5 µM DIN) are within the range of ~0.01-0.05 d^{-1}; however, these values are still higher than most specific growth rates reported in the literature, which are typically based on skeletal mass, and fall near or below 0.01 d^{-1} (Osinga et al. 2011; Osinga et al. 2012) (though values as high as 0.025 d^{-1} have been reported (Schutter et al. 2010)). These generally low skeletal growth rates relative to predicted biomass growth may be explained by differential substrate-limitation (i.e., CO_2 may limit calcification, which is not present in the model); indeed, tissue and skeletal growth may not always be well correlated (Anthony 2002). Furthermore, bioerosion may reduce net skeletal growth, especially in the field (Bak 1976). Nevertheless, when rates of increase in coral tissue biomass have been directly measured over short periods, values are consistent with model predictions (e.g., 0.07 d^{-1} in Tanaka et al. (2007)), and similar rates (0.04 d^{-1}) have been measured in *Aiptasia diaphana*, a non-calcifying symbiotic anemone (Armoza-Zvuloni et al. 2014).

As irradiance continues to increase above ~15-20 mol photons m^{-2} d^{-1}, growth rates decline until positive growth ceases above ~30 µmol photons m^{-2} d^{-1}. The mechanism underlying this decline is the increase in light energy beyond the capacity of photosynthesis and non-photochemical quenching: excess excitation energy generates reactive oxygen species (ROS) (Weis 2008; Roth 2014), which, in this model, have the phenomenological consequences of reducing the photosynthetic rate (representing photoinhibition) and increasing the symbiont biomass loss rate (representing photodamage and/or symbiont expulsion) (see Eynaud, Nisbet, and Muller 2011). Together, these impacts reduce the symbiont to host biomass ratio (Fig. 2C), as occurs during coral bleaching. This reduction in symbionts consequently reduces the flux of fixed carbon to the host, resulting in increasing carbon-limitation (Fig. 2B) and eventual cessation of growth (Fig. 2A). Importantly, these consequences arise in the present model only when light energy exceeds the capacity of photochemistry and NPQ, which in turn depends on CO_2 availability. While previous models framed photophysiological stress as a fixed response to absolute irradiance levels (Eynaud, Nisbet, and Muller 2011), the current implementation considers the dynamic balance of multiple energy sinks in the causation of stress, which is more consistent with current understanding of symbiosis dysfunction (Wooldridge 2013), and establishes an important role of the host in providing CO_2 for symbiont photosynthesis (Tansik, Fitt, and Hopkinson 2015; Hopkinson, Tansik, and Fitt 2015).

While bleaching in response to high light alone has been observed experimentally (Schutter et al. 2011; Downs et al. 2013), mass coral bleaching events occur in response to high temperature (Hoegh-Guldberg 1999); thus, it is important to justify our consideration of light as the primary stressor in the model. In reality, light and temperature interact synergistically (Coles and Jokiel 1978; Jones et al. 1998), and in fact, any stressor that disrupts the quenching of light energy may lead to bleaching (Wooldridge 2010; Baker and Cunning 2015). This is because the proximate cause of coral bleaching is excess excitation energy, but the upstream events that lead to this situation may be diverse: indeed, elevated temperature inhibits Rubisco functioning (Jones et al. 1998) and repair of the D1 protein in photosystem II (Warner, Fitt, and Schmidt 1999), which reduces the capacity of photochemical quenching and leads to an excess of light energy. In this way, elevated temperature serves to reduce the threshold above which light causes stress to the system (Hoegh-Guldberg 1999); importantly, light is still the proximate stressor. Therefore, we omitted temperature from the model, which serves to maintain a desired level of simplicity, while still allowing photophysiological stress and bleaching to be simulated with biological realism in response to light. Thus, the specific light levels that cause stress here should be interpreted in this context, and the effects of high light are analagous to the effects of high temperature.

The incorporation of light stress in the model sets an upper limit to the amount of light at which a stable symbiotic interaction can be maintained, but even below this threshold of breakdown, negative effects of high light reduce steady state growth and symbiont:host biomass (Fig. 2A,C). This gradual decline is consistent with experimental results showing that high light levels decrease growth (Schutter et al. 2011), and field studies documenting optimum growth rates at intermediate depths (Baker and Weber 1975; Huston 1985). Consequently, the model predicts greater variation in state variables across light gradients than was predicted by the model of Muller et al. (2009), which did not include photoinhibition and photodamage. It is important to recognize that these are steady state values predicted under a constant environment at the given light and nutrient levels; a dynamic system may temporarily cross this threshold and experience a period of symbiont loss (bleaching) and reduced growth, after which a return to benign conditions may restore symbiont biomass and positive growth. To explore this further and illustrate the behavior of the model in more detail, we evaluate a number of dynamic simulations below.

Dynamic behavior

varying light: consequences of excess light and light-limitation

varying DIN: role of N-limitation and consequences of elevated N

elevated nutrients cause system to become C-limited (photo: CO2 limited; host: fixed-C limited)

C-limitation increases susceptibility to bleaching

consequences of a less efficient but more tolerant symbiont

Rate of symbiont repopulation (Berner et al. 1993)

Bicarbonate addition promotes coral growth (Marubini and Thake 1999)

Seasonal change in sym. density is larger when nutrients are elevated (Stimson 1997). Such a phenomenon was predicted by Fitt et al. 2000.

Death rule: negative growth for a certain amount of time should be defensible.

References

Anthony, K. 2002. "Comparative analysis of energy allocation to tissue and skeletal growth in corals." *Limnology and Oceanography* 47 (5): 1417–29. https://www.scopus.com/inward/record.uri?partnerID=HzOxMe3b&scp=0036733455&origin=inward.

Anthony, Kenneth R N, and Ove Hoegh-Guldberg. 2003. "Variation in coral photosynthesis, respiration and growth characteristics in contrasting light microhabitats: an analogue to plants in forest gaps and understoreys?" *Functional Ecology* 17 (April): 246–59.

Armoza-Zvuloni, Rachel, Esti Kramarsky-Winter, Yossi Loya, Ami Schlesinger, and Hanna Rosenfeld. 2014. "Trioecy, a unique breeding strategy in the sea anemone Aiptasia diaphana and its association with sex steroids." *Biology of Reproduction* 90 (6). Society for the Study of Reproduction: 122–22. doi:10.1095/biolreprod.113.114116.

Bak, R. 1976. "The growth of coral colonies and the importance of crustose coralline algae and burrowing sponges in relation with carbonate accumulation." *Netherlands Journal of Sea Research* 10 (3): 285–337. doi:10.1016/0077-7579(76)90009-0.

Baker, Andrew C, and Ross Cunning. 2015. "Coral 'Bleaching' as a Generalized Stress Response to Environmental Disturbance." In *Diseases of Coral*, 396–409. Hoboken, NJ: John Wiley & Sons, Inc. doi:10.1002/9781118828502.ch30.

Baker, P, and Jon N Weber. 1975. "Coral growth rate: Variation with depth." *Earth and Planetary Science Letters* 27 (1): 57–61. doi:10.1016/0012-821X(75)90160-0.

Barott, Katie L, Alexander A Venn, Sidney O Perez, Sylvie Tambutte, and Martin Tresguerres. 2014. "Coral host cells acidify symbiotic algal microenvironment to promote photosynthesis." *Proceedings Of The National Academy Of Sciences Of The United States Of America*, December. National Acad Sciences, 201413483. doi:10.1073/pnas.1413483112.

Brown, Barbara E, R P Dunne, I Ambarsari, Martin Le Tissier, and U Satapoomin. 1999. "Seasonal fluctuations in environmental factors and variations in symbiotic algae and chlorophyll pigments in four Indo-Pacific coral species." *Marine Ecology Progress Series* 191: 53–69.

Coles, SL, and Paul L Jokiel. 1978. "Synergistic effects of temperature, salinity and light on the hermatypic coral Montipora verrucosa." *Marine Biology* 49: 187–95. http://www.springerlink.com/index/LU582837924G7674.pdf.

Costanza, R, R de Groot, and P Sutton. 2014. "Changes in the global value of ecosystem services." *Global Environmental Change* 26: 152–58. doi:10.1016/j.gloenvcha.2014.04.002.

Downs, C A, Kathleen E McDougall, Cheryl M Woodley, John E Fauth, Robert H Richmond, Ariel Kushmaro, Stuart W Gibb, Yossi Loya, Gary K Ostrander, and Esti Kramarsky-Winter. 2013. "Heat-Stress and Light-Stress

Induce Different Cellular Pathologies in the Symbiotic Dinoflagellate during Coral Bleaching." *PLoS ONE* 8 (12): e77173. doi:10.1371/journal.pone.0077173.

Edmunds, Peter J, Hollie M Putnam, Roger M Nisbet, and Erik B Muller. 2011. "Benchmarks in organism performance and their use in comparative analyses." *Oecologia* 167 (2): 379–90. doi:10.1007/s00442-011-2004-2.

Enríquez, Susana, Eugenio R Méndez, and Roberto Iglesias-Prieto. 2005. "Multiple scattering on coral skeletons enhances light absorption by symbiotic algae." *Limnology and Oceanography* 50 (4): 1025–32.

Eynaud, Yoan, Roger M Nisbet, and Erik B Muller. 2011. "Impact of excess and harmful radiation on energy budgets in scleractinian corals." *Ecological Modelling* 222 (7). Elsevier: 1315–22. http://www.sciencedirect.com/science/article/pii/S0304380011000263.

Ferrier-Pagès, Christine, Jean-Pierre Gattuso, S Dallot, and Jean Jaubert. 2000. "Effect of nutrient enrichment on growth and photosynthesis of the zooxanthellate coral Stylophora ...." *Coral Reefs*. http://www.springerlink.com/index/3DRC3K1Q57TPC0UT.pdf.

Fitt, William K, F K McFarland, Mark E Warner, and Geoff C Chilcoat. 2000. "Seasonal patterns of tissue biomass and densities of symbiotic dinoflagellates in reef corals and relation to coral bleaching." *Limnology and Oceanography* 45 (3): 677–85.

Glynn, Peter W, Juan L Maté, Andrew C Baker, and MO Calderón. 2001. "Coral bleaching and mortality in Panama and Ecuador during the 1997-1998 El Niño-Southern Oscillation event: Spatial/temporal patterns and comparisons with the 1982-1983 event." *Bulletin of Marine Science* 69 (1): 79–109.

Hoegh-Guldberg, Ove. 1999. "Climate change, coral bleaching and the future of the world's coral reefs." *Marine and Freshwater Research* 50 (November): 839–66.

Hopkinson, Brian M, Anna L Tansik, and William K Fitt. 2015. "Internal carbonic anhydrase activity in the tissue of scleractinian corals is sufficient to support proposed roles in photosynthesis and calcification." *The Journal of Experimental Biology*, April. The Company of Biologists Ltd, jeb.118182. doi:10.1242/jeb.118182.

Huston, M. 1985. "Variation in coral growth rates with depth at Discovery Bay, Jamaica." *Coral Reefs* 4 (1): 19–25. doi:10.1007/BF00302200.

Jager, Tjalling, Benjamin T Martin, and Elke I Zimmer. 2013. "DEBkiss or the quest for the simplest generic model of animal life history." *Journal of Theoretical Biology* 328: 9–18. doi:10.1016/j.jtbi.2013.03.011.

Jokiel, Paul L, and SL Coles. 1977. "Effects of temperature on the mortality and growth of Hawaiian reef corals." *Marine Biology* 43 (3): 201–8.

Jones, Ross J, Ove Hoegh-Guldberg, Anthony W D Larkum, and Ulrich Schreiber. 1998. "Temperature-induced bleaching of corals begins with impairment of the CO2 fixation mechanism in zooxanthellae." *Plant, Cell and Environment* 21 (12): 1219–30.

Kooijman, SALM. 2010. *Dynamic Energy Budget Theory for Metabolic Organization*. 3rd ed. Cambridge University Press.

Marcelino, Luisa A, Mark W Westneat, Valentina Stoyneva, Jillian Henss, Jeremy D Rogers, Andrew Radosevich, Vladimir Turzhitsky, et al. 2013. "Modulation of Light-Enhancement to Symbiotic Algae by Light-Scattering in Corals and Evolutionary Trends in Bleaching." *PLoS ONE* 8 (4): e61492. doi:10.1371/journal.pone.0061492.s008.

Marubini, F, and PS Davies. 1996. "Nitrate increases zooxanthellae population density and reduces skeletogenesis in corals." *Marine Biology* 127 (2): 319–28. http://www.scopus.com/inward/record.url?partnerID=yv4JPVwI&eid=2-s2.0-0030301761&md5=0971551a6865f30046294b9e17fb4081.

Muller, Erik B, Sebastiaan A L M Kooijman, Peter J Edmunds, Francis J Doyle, and Roger M Nisbet. 2009. "Dynamic energy budgets in syntrophic symbiotic relationships between heterotrophic hosts and photoautotrophic symbionts." *Journal of Theoretical Biology* 259 (1): 44–57. doi:10.1016/j.jtbi.2009.03.004.

Muller-Parker, Gisèle, Lawrence R McCloskey, Ove Hoegh-Guldberg, and PJ McAuley. 1994. "Effect of ammonium enrichment on animal and algal biomass of the coral Pocillopora damicornis." *Pacific Science* 48 (3).

http://scholarspace.manoa.hawaii.edu/handle/10125/2236.

Muscatine, Leonard, and James W Porter. 1977. "Reef corals: mutualistic symbioses adapted to nutrient-poor environments." *Bioscience* 27 (7): 454–60.

Muscatine, Leonard, L R McCloskey, and R E Marian. 1981. "Estimating the daily contribution of carbon from zooxanthellae to coral animal respiration." *Limnology and Oceanography* 26 (4): 601–11. doi:10.4319/lo.1981.26.4.0601.

Osinga, Ronald, Miriam Schutter, Ben Griffioen, René H Wijffels, Johan A J Verreth, Shai Shafir, Stéphane Henard, Maura Taruffi, Claudia Gili, and Silvia Lavorano. 2011. "The Biology and Economics of Coral Growth." *Marine Biotechnology* 13 (4): 658–71. doi:10.1007/s10126-011-9382-7.

Osinga, Ronald, Miriam Schutter, Tim Wijgerde, Buki Rinkevich, Shai Shafir, Muki Shpigel, Gian Marco Luna, et al. 2012. "The CORALZOO project: a synopsis of four years of public aquarium science." *Journal of the Marine Biological Association of the UK* 92 (04). Cambridge University Press: 753–68. doi:10.1017/S0025315411001779.

Powles, Stephen B. 1984. "Photoinhibition of photosynthesis induced by visible light." *Annual Review of Plant Physiology* 35: 15–44.

R Core Team. 2014. "R: A Language and Environment for Statistical Computing." Vienna, Austria: R Foundation for Statistical Computing. http://www.R-project.org/.

Roth, M S. 2014. "The engine of the reef: Photobiology of the coral-algal symbiosis." *Frontiers in Microbiology*. http://journal.frontiersin.org/Journal/10.3389/fmicb.2014.00422/pdf.

Schutter, M, J Crocker, A Paijmans, M Janse, R Osinga, A J Verreth, and R H Wijffels. 2010. "The effect of different flow regimes on the growth and metabolic rates of the scleractinian coral Galaxea fascicularis." *Coral Reefs*, April. doi:10.1007/s00338-010-0617-2.

Schutter, Miriam, Rosa M van der Ven, Max Janse, Johan A J Verreth, René H Wijffels, and Ronald Osinga. 2011. "Light intensity, photoperiod duration, daily light flux and coral growth of Galaxea fascicularis in an aquarium setting: a matter of photons?" *Journal of the Marine Biological Association of the UK* 92 (04). Cambridge University Press: 703–12. doi:10.1017/S0025315411000920.

Shantz, Andrew A, Nathan P Lemoine, and Deron E Burkepile. 2015. "Nutrient loading alters the performance of key nutrient exchange mutualisms." *Ecology Letters* 19 (1): 20–28. doi:10.1111/ele.12538.

Stimson, J. 1997. "The annual cycle of density of zooxanthellae in the tissues of field and laboratory-held Pocillopora damicornis (Linnaeus)." *Journal of Experimental Marine Biology and Ecology* 214 (1-2): 35–48.

Tanaka, Yasuaki, Akira Iguchi, Mayuri Inoue, Chiharu Mori, K Sakai, Atsushi Suzuki, Hodaka Kawahata, and Takashi Nakamura. 2013. "Marine Pollution Bulletin." *Marine Pollution Bulletin* 68 (1-2): 93–98. doi:10.1016/j.marpolbul.2012.12.017.

Tanaka, Yasuaki, Toshihiro Miyajima, Isao Koike, Takeshi Hayashibara, and Hiroshi Ogawa. 2007. "Imbalanced coral growth between organic tissue and carbonate skeleton caused by nutrient enrichment." *Limnology and Oceanography*. http://www.aslo.org/lo/toc/vol_52/issue_3/1139.pdf.

Tansik, Anna L, William K Fitt, and Brian M Hopkinson. 2015. "External carbonic anhydrase in three Caribbean corals: quantification of activity and role in CO2 uptake." *Coral Reefs* 34 (3). Springer Berlin Heidelberg: 703–13. doi:10.1007/s00338-015-1289-8.

Titlyanov, E A, T V Titlyanova, K Yamazato, and Robert van Woesik. 2001. "Photo-acclimation dynamics of the coral Stylophora pistillata to low and extremely low light." *Journal of Experimental Marine Biology and Ecology* 263 (2): 211–25.

Wang, J, and Angela E Douglas. 1998. "Nitrogen recycling or nitrogen conservation in an alga-invertebrate symbiosis?" *The Journal of Experimental Biology* 201: 2445–53.

Warner, Mark E, William K Fitt, and Gregory W Schmidt. 1999. "Damage to photosystem II in symbiotic dinoflagellates: A determinant of coral bleaching." *Proceedings Of The National Academy Of Sciences Of The*

United States Of America 96 (14): 8007–12.

Weis, Virginia M. 2008. "Cellular mechanisms of Cnidarian bleaching: stress causes the collapse of symbiosis." *The Journal of Experimental Biology* 211 (Pt 19): 3059–66. doi:10.1242/jeb.009597.

Wooldridge, Scott A. 2009. "A new conceptual model for the warm-water breakdown of the coral-algae endosymbiosis." *Marine and Freshwater Research* 60 (June): 483–96.

———. 2010. "Is the coral-algae symbiosis really 'mutually beneficial' for the partners?" *BioEssays*, May.

———. 2013. "Breakdown of the coral-algae symbiosis: towards formalising a linkage between warm-water bleaching thresholds and the growth rate of the intracellular zooxanthellae." *Biogeosciences* 10: 1647–58. http://www.biogeosciences.net/10/1647/2013/bg-10-1647-2013.html.

———. 2014a. "Differential thermal bleaching susceptibilities amongst coral taxa: re-posing the role of the host." *Coral Reefs* 33 (1). Springer Berlin Heidelberg: 15–27. doi:10.1007/s00338-013-1111-4.

———. 2014b. "Formalising a mechanistic linkage between heterotrophic feeding and thermal bleaching resistance." *Coral Reefs*. Springer Berlin Heidelberg, 1–6. doi:10.1007/s00338-014-1193-7.

Yellowlees, David, T A V Rees, and William Leggat. 2008. "Metabolic interactions between algal symbionts and invertebrate hosts." *Plant, Cell and Environment* 31: 679–94.

List of Figures

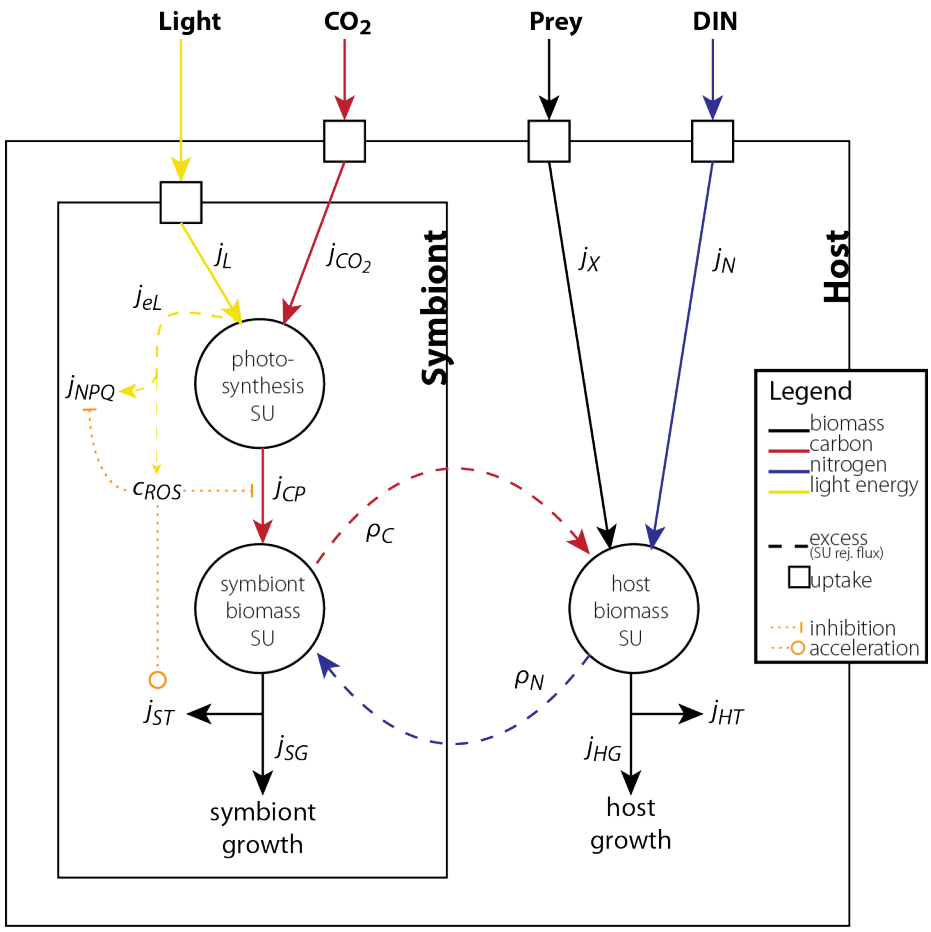

Figure 1: Graphical representation of coral-algal symbiosis model. Light, CO_2, prey, and DIN are acquired from the external environment proportional to the biomass of the partner indicated by the black box for uptake. Mass fluxes (see Table 1 for definitions) are represented by j's with subscripts indicating the type of mass, and in some cases the process (e.g., j_{CP} is the flux of carbon produced by photosynthesis), and ρ's indicate fluxes that are shared by one partner with the other. Parallel complementary synthesizing units (SUs) are represented by large circles, and rejection fluxes from these SUs are indicated by dashed lines. c_{ROS} is a proportional rate that impacts other model fluxes by inhibition or acceleration. Recycled mass fluxes from biomass turnover are not shown for clarity (but see Table 1 for definitions).

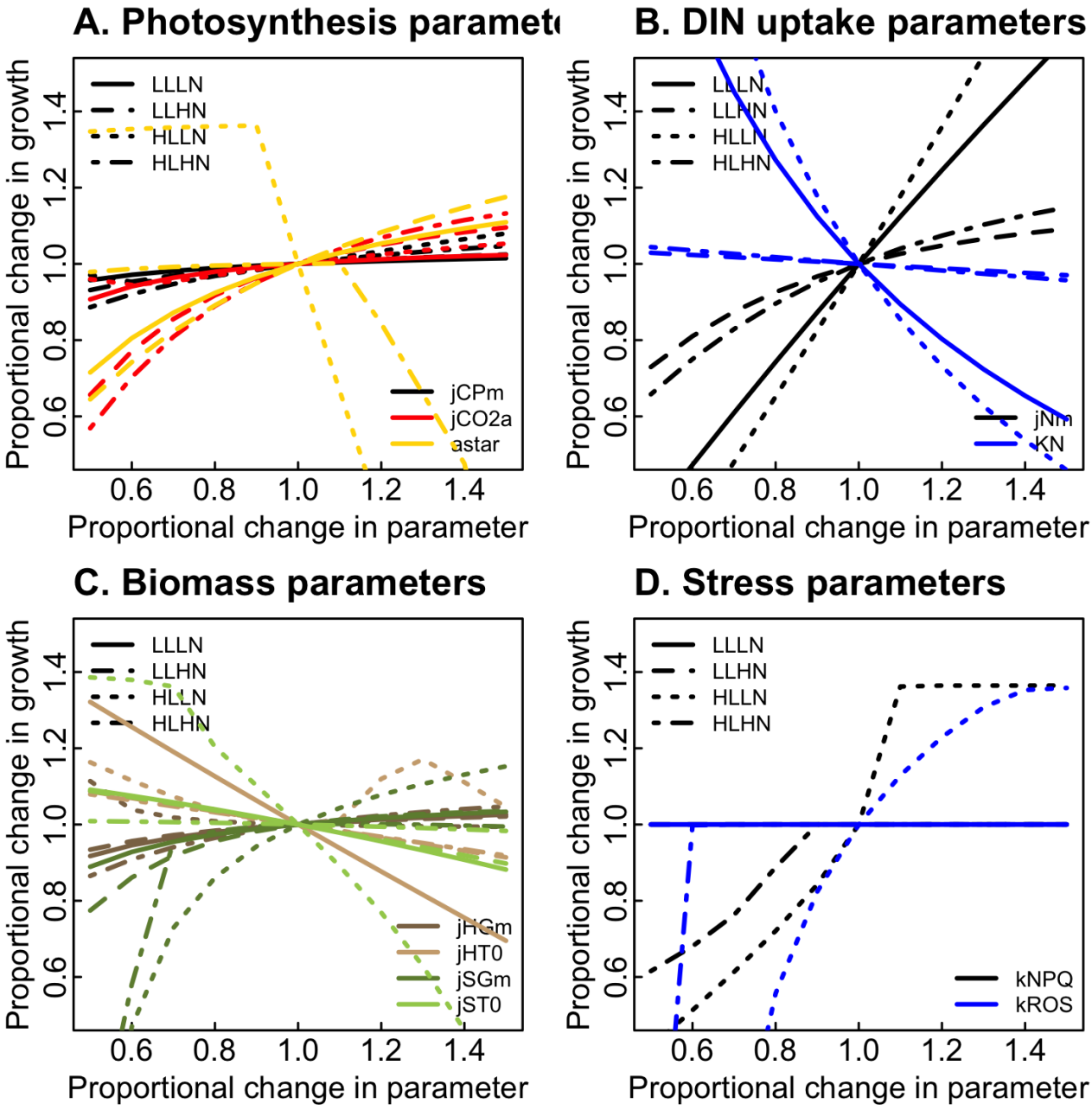

Figure 2: Sensitivity analysis. Plots show the fractional change in steady state values in response to fractional changes in default parameter values (see Table 2 for default values). Parameters are grouped by which processes they are involved in. Sensitivity in response to changes in each parameter was evaluated in each of four environments (indicated by line type): 1) LLLN=low light (2 mol ph m^{-2} d^{-1}) and low DIN (1e-7 mol L^{-1}), 2) LLHN=low light (2 mol ph m^{-2} d^{-1}) and high DIN (4e-6 mol L^{-1}), 3) HLLN=high light (30 mol ph m^{-2} d^{-1}) and low DIN (1e-7 mol L^{-1}), and 4) HLHN=high light (30 mol ph m^{-2} d^{-1}) and high DIN (4e-6 mol L^{-1}).

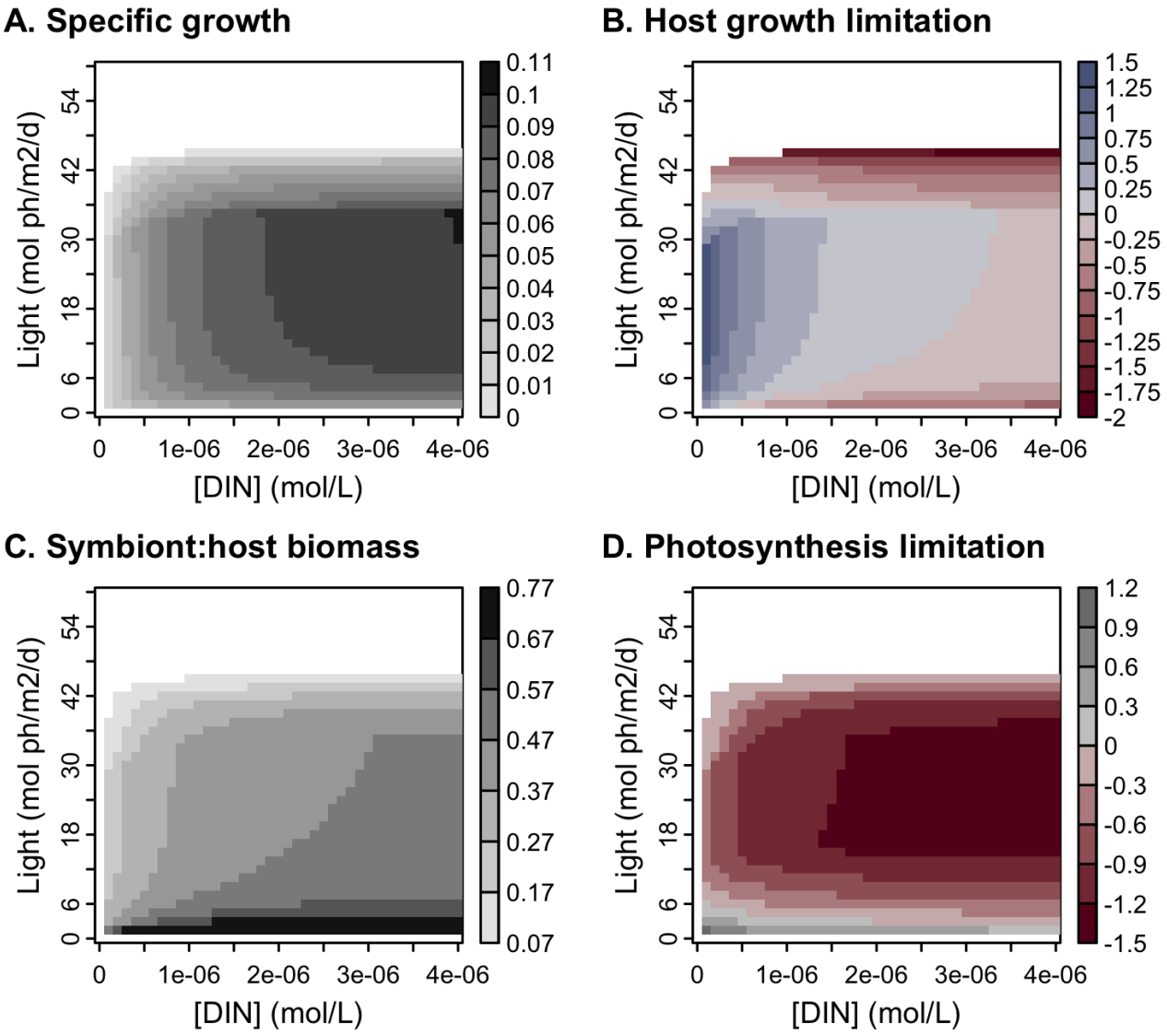

Figure 3: Steady state values of **A)** specific growth (Cmol Cmol^{-1} d^{-1}), **B)** the symbiont to host biomass ratio (CmolS CmolH^{-1}), **C)** relative C- or N-limitation of host biomass formation, and **D)** relative CO_2- or light-limitation of symbiont photosynthesis, across gradients of external irradiance and dissolved inorganic nitrogen. Note that typical conditions for reefs are ~1e-7 M DIN and 10-20 mol photons m^{-2} d^{-1}. Simulations for each combination of light and nutrients (41 points along each axis) were run for 100 days with a time step of 1 day. Negative steady state growth rates, and corresponding S:H ratios, were set to zero.